Cold Regions Science and Technology 153 (2018) 144–155

Contents lists available at ScienceDirect

Cold Regions Science and Technology

journal homepage: www.elsevier.com/locate/coldregions

Quantitative evaluation of glacier change and its response to climate change in the Chinese Tien Shan

Yanjun Che[a,b], Mingjun Zhang[a,*], Zhongqin Li[a,c], Shengjie Wang[a,c], Mingxia Du[a], Puyu Wang[c], Jie Wang[a], Panpan Zhou[a]

[a] College of Geography and Environmental Science, Northwest Normal University, Lanzhou 730070, Gansu, China
[b] Department of Geography Science, Yichun University, Yichun 336000, Jiangxi, China
[c] State Key Laboratory of Cryospheric Sciences, Northwest Institute of Eco-Environment and Resources/Tianshan Glaciological Station, Chinese Academy of Sciences, Lanzhou 730000, Gansu, China

ARTICLE INFO

Keywords:
Glacier change
Equilibrium Line Altitude (*ELA*)
Climate change
Chinese Tien Shan

ABSTRACT

Glacier melt water is an important water resource in arid regions of central Asia during the dry seasons, and it is very susceptible to climate disturbances. In this paper, based on the glacier datasets of the first and second Chinese Glacier Inventories, the glacier change in the Chinese Tien Shan from 1960s to 2010 was quantify by assessing the Annual Percentages of Area Changes (*APAC*), Annual Percentages of Volume Changes (*APVC*), and Equilibrium Line Altitude (*ELA*). The results indicated that the mean glacier area and mean glacier volume decreased by 0.7% ± 0.6% per year and 0.83% ± 0.73% per year in the Chinese Tien Shan during the period of 1960–2010, respectively. The mean *ELA* increased by 24.87 ± 126.84 m during the study period. In addition, we also found that the glacier retreat in the Bogda Mountains was the fastest, mainly due to the sensitivity of small glaciers to climate change, with an *APAC* of −0.86% ± 0.49% per year and *APVC* of −1.04% ± 0.55% per year, and the mean *ELA* increased by 44.35 ± 55.07 m. Moreover, increases in both air temperature (in terms of Thawing Degree-Day (TDD) and Freezing Degree-Day (FDD)) and precipitation were found over the study area during the past five decades. However, such increases in precipitation did not result in any significant changes in the ratio of annual snowfall to total precipitation (S/P) across the Chinese Tien Shan Mountains. Hence, the glacier shrinkage mainly resulted from the significant increase in TDD and FDD in the study region.

1. Introduction

Glacial melt is an important hydrological process in High Mountain Asia, and changes in temperature and precipitation are expected to affect the melt characteristics (Aizen et al., 1997; Immerzeel et al., 2010; Kraaijenbrink et al., 2017; Sorg et al., 2012). A study in the Sary-Djaz-Kumaric River Basin of Tien Shan indicated that glacier melt increased by 5.4% in summer during the period of 1961–2005, 5.0% of which was due to rising temperature and only 0.4% due to increasing precipitation (Wang et al., 2015a, 2015b). Tien Shan is also known as the “water tower” in central Asia due to wide distribution of glaciers and snow (Immerzeel and Bierkens, 2012; Jansson et al., 2003; Kaser et al., 2010; Viviroli et al., 2007). Additionally, the melt-water from glaciers and snow in mountain ranges is an essential freshwater resource, especially if downstream climates are arid, water demands are high and glaciers are abundant during the summer (Immerzeel et al., 2015). However, due to the average increase in air temperature, it was generally accepted that the glaciers widely retreated in area, mass, and ice volume in the Tien Shan Mountains during the past several decades (Aizen et al., 1997; Bolch, 2007; Farinotti et al., 2015; Li et al., 2016; Sakai et al., 2015). Therefore, it is necessary to understand the response of glacier variation to climate change by determining the relationships between glacier change and climatic signals (e.g., air temperature and precipitation) (Kenzhebaev et al., 2017; Oerlemans et al., 1998).

The changes in glacier area and volume in the Tien Shan Mountains have been understood in recent decades (e.g., Aizen et al., 2006; Farinotti et al., 2015; Li et al., 2004; Li et al., 2010; Li et al., 2011; Pieczonka and Bolch, 2015; Pieczonka et al., 2013). For example, based on the topographic maps, the Digital Elevation Data from Shuttle Radar Topography Mission (SRTM DEM) and Advanced Space borne Thermal Emission and Reflection Radio meter (ASTER) images, Aizen et al. (2006) found that the glacier areas of Akshiirak and Ala Archa in the central Tien Shan Mountains decreased by 12.9% and 15.7% during the period of 1943–2003, respectively. He et al. (2015) reported that glacier area decreased by 0.81% per year on average in Tomur Peak, Alatau, Nalati, Tianger, and Harlik (excluding Barkol) Mountains of the

* Corresponding author.
E-mail address: mjzhang2004@163.com (M. Zhang).

https://doi.org/10.1016/j.coldregions.2018.05.010
Received 1 November 2017; Received in revised form 7 May 2018; Accepted 31 May 2018
Available online 01 June 2018
0165-232X/

Chinese Tien Shan from 1990 to 2011.

It is noted that glacier mass balance is a direct, undelayed signal of climatic change; however, the number of glaciers with an observed mass balance is very low. In general, an assumed step change in the equilibrium line altitude (*ELA*) induces an immediate step change in specific mass balance (Haeberli, 1998). The resulting specific mass balance is the outcome of the shift in equilibrium line altitude (ΔELA) and the gradient of mass balance with altitude as weighed by the distribution of glacier surface area with altitude (hypsometry). The hypsometry represents the local/individual or topographic part of the glacier sensitivity, whereas the mass balance gradient mainly reflects the regional or climatic part. The *ELA* is best determined by careful measurements of mass balance stakes and snow pits on the glacier surface; then, the isolines of the zero balance may be drawn, and their altitude is called *ELA* (Braithwaite and Müller, 1980; Hewitt and Young, 1990; Hock and Jensen, 1999; Østrem and Brugman, 1991). Therefore, glacier mass balance is zero at the equilibrium line, and then, the *ELA* is also widely used to study the relationship between glaciers and climate change (Mukhopadhyay and Khan, 2017). In addition, the *ELA* is sensitive to perturbations in either precipitation and air temperature; for example, it increases in response to decreasing snowfall and/or increasing frequency of positive air temperatures, and vice versa (Benn and Lehmkuhl, 2000).

As few glaciers can be measured directly in terms of in situ *ELA*, alternative approaches to estimate *ELA* are needed to quickly assess glacier change (Braithwaite and Müller, 1980; Braithwaite and Raper, 2009; Ding and Xie, 1991). For example, the *ELA* of the Last Glacial Maximum in northwest Barguzinsky of Northern Baikal was reconstructed using four common methods (Osipov, 2004): the median elevation of glacier (Meierding, 1982); accumulation area ratio, which is defined as the ratio of the accumulation area to the total glacier area (Meier and Post, 1962); toe-head wall altitude ratio, which is introduced in detail in section "2.5 Toe-to-Headwall Altitude Ratio (THAR)" (Porter, 1981); and Gefer's method, which indicated that the *ELA* can be determined as the arithmetic mean between the elevation of the lowest point of a glacier and the mean elevation of mountain summits surrounding its field (Kalesnik, 1963). These methods are generally used to calculate the *ELA* when no direct *ELA* data of in situ mass balance are obtained. Accordingly, they are widely adopted to assess the relationship between modern glaciers and climate change (e.g., Cui and Wang, 2013; Osmaston, 2005; Sakai et al., 2015).

As a consequence, glacier changes are among the clearest signals of the ongoing warming trends existing in nature (Haeberli, 1998). When climate changes, the energy/mass balance in a glacier changes first, and it is a direct/undelayed signal; then, the geometry/temperature of a glacier changes. In the end, these changes lead to glacier advance or retreat, which are indirect/delayed signals and show a time interval between climate change and glacier advance or retreat (Haeberli et al., 1989; Wood, 1990). Therefore, glacial parameters, such as glacier area, glacier volume, and glacier elevation, can be used to understand the response of glaciers to climate change. However, few glaciers have been studied in situ. To investigate the general characteristics of the existing glaciers in China, the compilation of the first Chinese Glacier Inventory (CGI-1) was carried out by Chinese glaciologists during the period 1978–2002 (Shi et al., 2009). These data were finally released in the early 2000s, and the results were also submitted to the International Commission on Snow and Ice for a World Glacier Inventory (WGI). After that, to have new and complete knowledge of glacier changes, the compilation of the second Chinese Glacier Inventory (CGI-2) was also initiated in 2007 and released in 2014 (Guo et al., 2014, 2015). The two surveys indicated that the glaciers in China have significantly retreated during the past several decades, and they provided the chance to quantify the glacier changes at a large scale (Liu et al., 2015).

In the Chinese Tien Shan, most works on the glacier change have mainly focused on the problems of one or several glaciers/glacierized basins (e.g., Farinotti et al., 2015; He et al., 2013a, 2013b; He et al., 2015; Huai et al., 2014; Zhu et al., 2014). For example, Farinotti et al. (2015) studied the glacier change in the Tien Shan and indicated that glacier area decreased by 18 ± 6% from 1961 to 2012. Due to the lack of Chinese glacier data, their study did not include the glaciers in the eastern regions of the Bogda Mountains, i.e., the eastern Bogda, Barkol, and Harlik Mountains, located in the eastern Chinese Tien Shan. Fortunately, the CGI-2 provides many glacial parameters, such as glacier area, length, and elevation (see in section "2.2 Glacier Datasets"), which are useful to understand the glacier behaviour during the past five decades.

The basic character and total decrease of glaciers (e.g., changes in number and area) can be quickly realized based on the two CGIs. However, how the glacier changes and the reasons for change in the Chinese Tien Shan during the past several decades are still unclear, such as the rates of glacier change and *ELA* shift. In addition, the spatial pattern of glacier change and how climate change affects these patterns, which are very important, are addressed in this paper. Herein, based on the datasets of the two CGIs, we will assess the glacier change and link it to the climate change according to the following order: "Glacier retreat-ELA shift-Climate change". The assessment of glacier change, i.e., the rate of change in area/volume and *ELA* shift, and the cause of glacier change in the Chinese Tien Shan are the main aims with respect to this paper. For the aims, we first calculated the rate of glacier change in the Chinese Tien Shan by the two glacial parameters, i.e., Annual Percentages of Area Changes (*APAC*) and Annual Percentages of Volume Change (*APVC*). After that, the *ELAs* of glaciers are assessed based on the two methods of using the Median Elevation of the Glacier and using the toe-to-headwall altitude ratio. To understand the spatial discrepancies in glacier retreat, the study area was divided into five sub-regions. In addition, the meteorological datasets of air temperature and precipitation will be used to interpret the cause of glacier retreat in the Chinese Tien Shan.

2. Description of study area, datasets, and methods

2.1. Study area

Tien Shan is located in the arid region of central Asia, running approximately 2400 km from west to east, and the eastern 1700 km is located in China. The eastern end of the Tien Shan is usually understood to be east of Urumqi in Western cartography, and this range is widely used by some studies (e.g., Farinotti et al., 2015; Kenzhebaev et al., 2017; Sorg et al., 2012). In Chinese cartography, however, the Tien Shan also includes the Bogda, Barkol, and Harlik Mountains (excluded in Western cartography). In this paper, our study focused on glaciers in the Chinese Tien Shan, including glaciers in the Bogda, Barkol, and Harlik Mountains. It is acknowledged that high mountains of the Chinese Tien Shan can obstruct the moisture of mid-latitude westerlies to form precipitation (Bothe et al., 2010; Bothe et al., 2012; Yao et al., 2012). In addition, the interaction between the westerly disturbance and the atmospheric circulation from the Siberian high can also trigger the precipitation in mountain landforms (Aizen et al., 1995). Accordingly, the precipitation in high mountains is usually greater than that in plains of the Chinese Tien Shan. To understand the spatial difference of glacier change in this paper, the glacierized region was divided into five sub-regions following the traditional method of glacier research in China (Shi et al., 1988), i.e., the South Chinese Tien Shan (R1), Middle Chinese Tien Shan (R2), North Chinese Tien Shan (R3), Bogda (R4), and Harlik (R5) Mountain as shown in Fig. 1. There were 7934 glaciers distributed in the Chinese Tien Shan following the dataset of CGI-2 (Liu et al., 2015), and 5700 glaciers with a total area of 3281.06 km^2 were used to assess glacier change in the Chinese Tien Shan Mountains in this paper. The median elevations of the glaciers range from approximately 3000 m a.s.l to 5500 m a.s.l. and glacier areas $\leq 50\ km^2$ are mostly distributed at approximately 4000 m a.s.l.

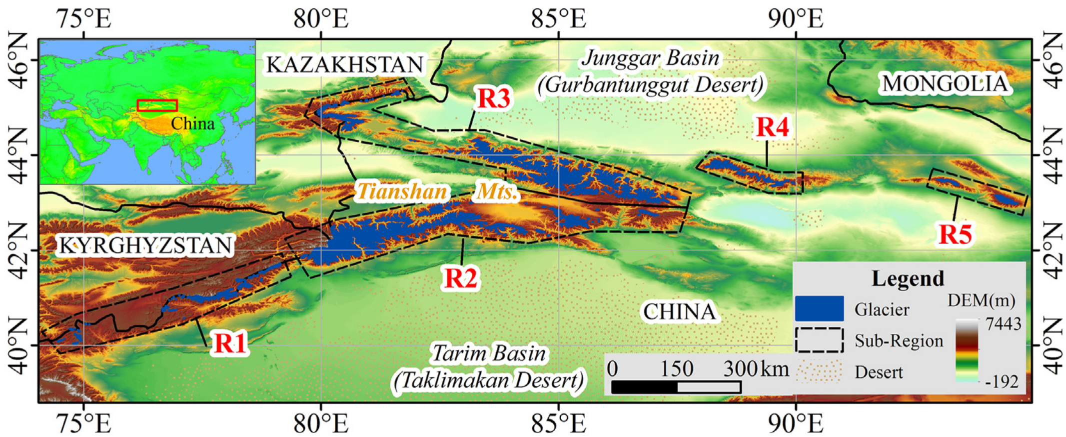

Fig. 1. Map showing the distribution of glaciers in the Chinese Tien Shan. The Chinese Tien Shan Mountains were divided into five sub-regions, i.e., R1: South Chinese Tien Shan, R2: Middle Chinese Tien Shan, R3: North Chinese Tien Shan, R4: Bogda Mountains, and R5: Harlik Mountains. The distribution of deserts in China is based on Wang et al. (2005).

2.2. Glacier datasets

The glaciers in the Chinese Tien Shan Mountains have been compiled in some glacier inventories, such as the World Glacier Inventory (WGI) (WGMS, National Snow and Ice Data Center (NSIDC), 1999), Global Land Ice Measurement from Space (GLIMS) (Bishop et al., 2004), and Randolph Glacier Inventory (RGI) (RGI, 2017). The CGI-2 is the currently the most recent and authoritative in terms of glacier data in the Chinese Tien Shan. The two datasets of CGIs are available online at the Cold and Arid Regions Science Data Center at Lanzhou (*http://westdc.westgis.ac.cn*).

When determining the relationship between glacier data from the CGI-1 and CGI-2, we found some mismatches of specific glaciers. For example, (I) some glaciers of CGI-2 were not compiled in the work of CGI-1; however, these glaciers did not form in recent decades. (II) One glacier in CGI-1 was divided into two or more parts due to glacier retreat. Each separate part of the glacier has its own characteristics of glacier movement and independent response to climate change; for example, the Urumqi Glacier No. 1 was separated into two glaciers (the eastern and western branches) in 1993. (III) Some small glaciers in CGI-1 entirely disappeared (Xu et al., 2015), but the accurate date of glacier disappearance was not precisely confirmed. (IV) The area variations of some glaciers were statistically anomalous (e.g., increased or decreased by many times the original area in CGI-1). This is possibly related to glacier dynamics, such as avalanche or glacier surge (Gardelle et al., 2012; Quincey et al., 2011), but the underlying reason is difficult to confirm on a case-by-case basis. These factors may be little help in investigating the changes of glacier resources, while greatly impacting the calculation of the rate of glacier change. For example, one glacier existed in CGI-1 and disappeared, and it is not found until the investigation of CGI-2. We can know the decreased glacier area, while how long it existed and when it disappeared are not confirmed. To accurately calculate the rate of glacier retreat in the Chinese Tien Shan during recent decades, mismatched information must be considered. Hence, we only chose glaciers without mismatched information, and 5700 glaciers were considered in this paper. In addition, as it is difficult to obtain the images covering the study area at the same time, the investigation time for glacier inventory is usually defined as a period spanning several years. The imaging times of most glaciers in CGI-1 were during the period 1960–1965, while those in CGI-2 were during the period 2006–2010 in terms of the Chinese Tien Shan. Accordingly, the glacier changes between the two inventories are expressed as glacier change from the 1960s to 2010 in this paper.

2.3. Glacier area and volume

The Annual Percentage of Area Changes (*APAC*) has been widely used to assess changes in glacier area over time (e.g., Ding et al., 2006; Nie et al., 2010; Zhang et al., 2011), and the formula is:

$$APAC = \frac{\Delta S}{S_1 \Delta t} \tag{1}$$

where *APAC* is the annual percentage of area change, S_1 is the area of the glacier in the 1960s (i.e., CGI-1), $\Delta S = S_2 - S_1$ is the change in area of the glacier during the study period, S_2 is the area of the glacier in 2010 (i.e., CGI-2), and $\Delta t = 50$ years is the time span of the study period.

In addition, the volume-area scaling was used in some previous studies (e.g., Bahr, 1997; Erasov, 1968; Radić et al., 2007, 2008; Radić and Hock, 2010) to calculate the volumes of glaciers:

$$V = cA^{\gamma} \tag{2}$$

where V and A are volume and area of a single glacier, while c and γ are scaling parameters of the glacier. Bahr (1997) determined $\gamma = 1.375$ and $c = 0.191\ \mathrm{m}^{3-2\gamma}$ for mountain glaciers based on theoretical considerations, while Chen and Ohmura (1990) confirmed $c = 0.2055\ \mathrm{m}^{3-2\gamma}$ when $\gamma = 1.36$ for 63 mountain glaciers. Radić and Hock (2010) calculated the regional and global ice volumes from regional glacier area data of WGI using Eq. (2) with $c = 0.2055\ \mathrm{m}^{3-2\gamma}$ and $\gamma = 1.375$. In their study, the regions of glacier distribution referred to 19 regions globally, including North and East Asia, High Mountain Asia, and Central Europe. In addition, the errors of scaling coefficients γ and c were also assessed, which indicated that the uncertainties of volume-area scaling, including the values of γ and c, were acceptable for the assessment of regional and global glacier resources. Here, we adopted $\gamma = 1.375$ and $c = 0.2055\ \mathrm{m}^{3-2\gamma}$ to calculate the volume of each glacier in this paper. Similar to *APAC*, the Annual Percentage of Volume Change (*APVC*) in unit time was defined as:

$$APVC = \frac{\Delta V}{V_1 \Delta t} \tag{3}$$

where *APVC* is the annual percentage of volume change for a single glacier, V_1 is the volume of the glacier in the 1960s, $\Delta V = V_2 - V_1$ is the change in volume of the glacier from CGI-1 to CGI-2, V_2 is the volume of the glacier in 2010, and $\Delta t = 50$ years is the time span of the study period in this paper.

2.4. Median Elevation of the Glacier

The Median Elevation of the Glacier (MEG) is a key parameter in the glacier inventory database and is often used for quick *ELA* estimates (Braithwaite and Raper, 2009; Meierding, 1982). Ding and Xie (1991) and Xie et al. (1996) noted that the MEG was approximately equal to the *ELA* deduced by mathematical theory. They also compared MEG to *ELA* for 16 reference glaciers, which showed high correlations. Sakai et al. (2015) found that the decadal *ELA*s were in accordance with the MEGs of glaciers in High Mountain Asia. Here, we assumed that the MEGs could be used as a proxy for the *ELAs* of glaciers in the Chinese Tien Shan Mountains. The MEGs of glaciers in the Chinese Tien Shan Mountains were derived from the datasets of CGI-1 and CGI-2 in this paper.

2.5. Toe-to-Headwall Altitude Ratio (THAR)

Generally, *ELA* is defined as a function of glacier elevation, and it can be rapidly calculated by (Aa, 1996; Murray and Locke III, 1989; Osipov, 2004; Porter, 1981; Torsnes et al., 1993):

$$ELA = E_{\min} + \Delta E \times r \tag{4}$$

where *ELA* and $E_{\min}$ are the equilibrium line altitude and minimum elevation of a glacier, respectively, ΔE is the vertical range between the maximum and minimum elevation of a glacier (i.e., $\Delta E = E_{\max} - E_{\min}$), and r is a ratio between the maximum and minimum altitude of a glacier. This method is generally called the "Toe-to-Headwall Altitude Ratio" (THAR). Murray and Locke III (1989) found through calculation that the ratios of 0.35–0.40 were the best parameters. Torsnes et al. (1993) and Aa (1996) took the ratio of 0.40 to calculate the *ELA*s of glaciers, while Osipov (2004) used the ratio of 0.42. The ratios ranged from 0.35 to 0.42, and the variations mainly depend on the continental degree of the local conditions (Osipov, 2004). In this paper, the ratio (r) of 0.42 was adopted to calculate the *ELA*, and the results of calculated *ELA* were compared with the widely used MEG in the 1960s and 2010.

2.6. Meteorological datasets

In this paper, the daily air temperature and precipitation datasets (SURF_CLI_CHN_PRE_DAY_GRID_0.5 and SURF_CLI_CHN_TEM_DAY_RID_0.5) at spatial resolutions of 0.5° × 0.5° were used to assess the climate change across the Chinese Tien Shan. The datasets derived from the China Meteorological Data Sharing Service System (*http://data.cma.cn/*), which were made from the spatial interpolation of the Thin Plate Spline based on the > 2470 meteorological stations in China since 1961, were used (NMIC, 2012a, 2012b). The quality of the two datasets was very high and was assessed by the organization publishing the data (NMIC, 2012a, 2012b) and Zhao and Zhu (2015). In recent years, the datasets have been widely applied to study climate change in China (e.g. Dong et al., 2014; Lin et al., 2015; Ren et al., 2015; Shen et al., 2015; Wang et al., 2013). For instance, Wang et al. (2016a, 2016b) described the change in snowfall on the Tibetan Plateau based on the datasets of daily air temperature and precipitation.

2.7. Trend analysis methods

When studying the change in climatologic time series, the detection of significant trends is usually tested. In this paper, two non-parametric methods, i.e., the Mann-Kendall trend test and Sen's slope estimator, were used to detect the meteorological variable trends in the Chinese Tien Shan.

2.7.1. Mann-Kendall trend test

The Mann-Kendall trend test (Kendall, 1975; Mann, 1945) has been widely used to quantify the significance of trends in meteorological time series (e.g., Douglas et al., 2000; Gocic and Trajkovic, 2013; Partal and Kahya, 2006; Salami et al., 2016; Tabari and Marofi, 2011; Yang and Tian, 2009). The Mann-Kendall test is calculated by the formulations below:

$$S = \sum_{i=1}^{n-1} \sum_{j=i+1}^{n} \operatorname{sgn}(x_j - x_i) \tag{5}$$

$$\operatorname{sgn}(x_j - x_i) = \begin{cases} +1, & \text{if } x_j - x_i > 0 \\ 0, & \text{if } x_j - x_i = 0 \\ -1, & \text{if } x_j - x_i < 0 \end{cases} \tag{6}$$

$$Var(s) = \left[\frac{1}{18} \left(n(n-1)(2n+5) - \sum_{i=1}^{m} t_i(t_i - 1)(2t_i + 5) \right) \right] \tag{7}$$

$$Z_s = \begin{cases} \frac{S-1}{\sqrt{Var(s)}}, & \text{if } S > 0 \\ 0, & \text{if } S > 0 \\ \frac{S+1}{\sqrt{Var(s)}}, & \text{if } S < 0 \end{cases} \tag{8}$$

where S is the Mann-Kendall test statistic value, n is the number of data points, x_i and x_j are the values in time series i and j ($j > i$), respectively, $\operatorname{sgn}(x_j - x_i)$ denotes the sign function of $(x_j - x_i)$, m is the number of tied groups, and t_i denotes the number of ties of extent i; a tied group is a set of sample data with the same value. The statistic Z_s is calculated by Eqs. (5) and (7). Positive values of Z_s indicate increasing trends, while negative Z_s values show decreasing trends. The trend test is conducted with a specific α significance level. When $|Z_s| > Z_{1-\alpha/2}$, the null hypothesis is rejected, and a significant trend exists in the time series, and vice versa. In this work, the significance level $\alpha = 0.5$ (i.e., the 5% significance level) was used. That is, the null hypothesis of a non-significant trend is rejected if $|Z_s| > 1.96$ at the 5% significance level.

2.7.2. Sen's slope

Sen (1968) developed the non-parametric procedure for estimating the slope of a trend in a sample of N pairs of data, which was frequently used in meteorological time series (e.g., Lettenmaier et al., 1994; Gocic and Trajkovic, 2013; Partal and Kahya, 2006; ElNesr et al., 2010). The slope of any two values in observational data is expressed as:

$$L_i = \frac{x_j - x_k}{j - k}, \text{ if } i = 1, 2, \ldots, N \tag{9}$$

where x_k and x_j are the data values at times k and j ($j > k$), respectively.

If there is only one datum in each time period, then $N = n(n-1)/2$, where n is the number of time periods. If there are multiple observations in one or more time periods, then $N < n(n-1)/2$, where n is the total number of observations. Therefore, the N values of L_i are ranked from smallest to largest, and the median slope value, i.e., Sen's slope estimator, is computed as:

$$L_{med} = \begin{cases} L_{[(N+1)/2]}, & \text{if } N \text{ is odd} \\ \frac{1}{2}\{L_{[N/2]} + L_{[(N+2)/2]}\}, & \text{if } N \text{ is even} \end{cases} \tag{10}$$

L_i reflects the data trend and the slope of its trend, which is also tested at a specific probability to obtain the confidence interval. In this study, the Mann-Kendall trend test and Sen's slope estimator are jointly used to assess the trends in meteorological variations. Likewise, the statistical test at a significance level $\alpha = 0.5$ was used.

3. Results

3.1. General characteristics of glaciers

As mentioned above, 5700 glaciers in CGI-1 and CGI-2 were used, respectively, and they corresponded one-by-one with the glaciers measured from the 1960s to 2010. As shown in Fig. 2a, there were 1829

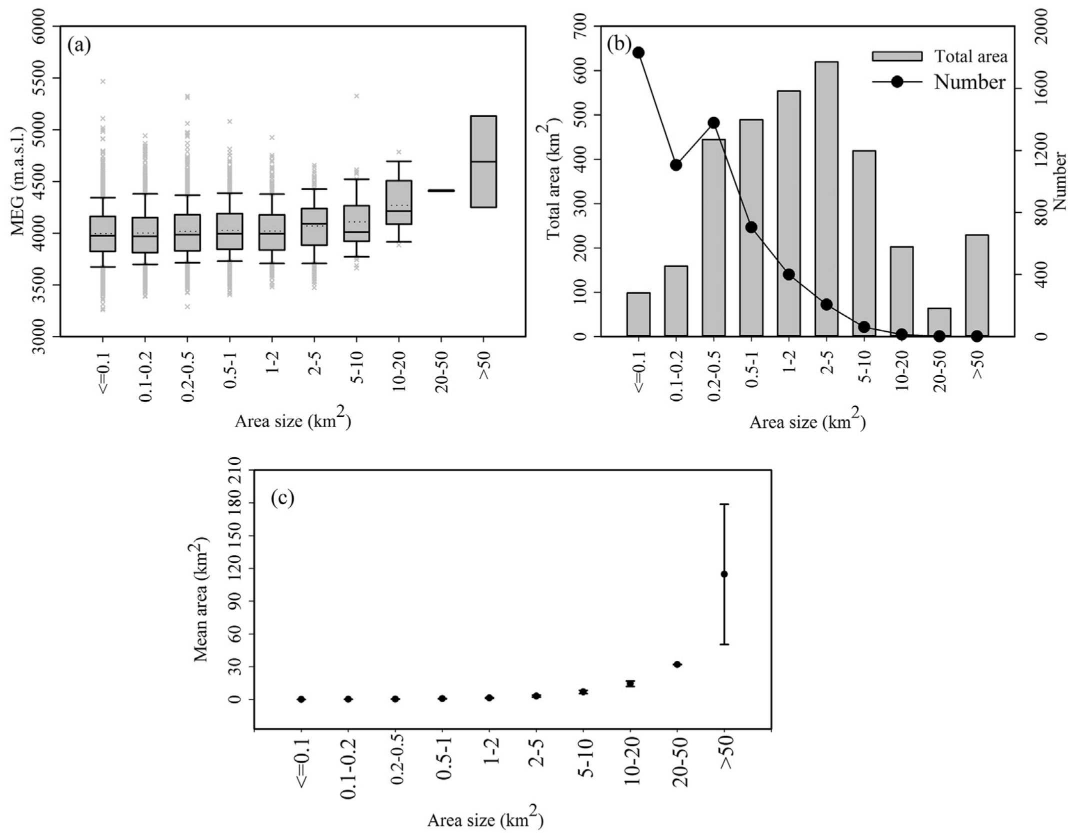

Fig. 2. Box plots showing the variations in MEG (a), total area and number (b), and mean area (c) for each size class. In plot (a), the lower boundary of the box indicates the 25th percentile, the upper boundary of the box indicates the 75th percentile, the dashed line in the box is the mean value, the solid line within the box marks the 50th percentile (median), whiskers below and above the box present the 10th and 90th percentiles, respectively, and crosses below and above whiskers indicate outliers. In plot (c), error is the standard deviation.

glaciers (32.09% of the total) with areas < 0.1 km^2, and the sum of their area was 98.81 km^2 (3.01% of the total area) (Fig. 2b). The glaciers with areas ranging from 0.2 km^2 to 10 km^2 accounted for 77.02% of the total, while their number accounted for 48.21%. There were 5015 glaciers (87.98% of the total number) with areas ≤1 km^2 (36.33% of the total area). There was only one glacier (160.03 km^2, CGI-2 code: 5Y673K0001, GLIMS-ID: G080211E42128N) where the area was > 100 km^2. Therefore, the existing glaciers in the Chinese Tien Shan were dominated by small glaciers with glacier areas ≤1 km^2. In addition, the mean area of glaciers with different sizes can be clearly seen in Fig. 2c.

3.2. The changes in glacier area and volume

During the period of the 1960s-2010, 90.72% (5171 glaciers) of the total number of glaciers showed decreases in terms of area in the Chinese Tien Shan, while other glaciers increased in area (Fig. 3a). Additionally, the same number of glaciers decreased in terms of glacier volume using the volume-area scaling (Fig. 3b). In addition, spatial discrepancies of glacier change were significant. Though a small number of glaciers were enlarged in some places, especially in the region of R2, most glaciers presented shrinkage during the study period. To assess the relative rate of glacier area change, the *APAC* of each glacier was calculated. The results showed that the *APAC* of glaciers in the whole region was −0.7% ± 0.6% per year (arithmetic mean ± standard deviation) (Table 1). To understand the spatial discrepancy in terms of the glacier change, those in the five sub-regions were analysed. The strongest relative decrease was found at sub-region R4 with an *APAC* of −0.86% ± 0.49% per year, while the weakest relative decrease was located in sub-region R1 with an *APAC* of −0.61% ± 0.61% per year.

In addition, the volume of glaciers in the Chinese Tien Shan had decreased on average by 0.83% ± 0.73% per year (Fig. 3b). Likewise, the *APVCs* of each glacier in the five sub-regions were also calculated. The results suggested that the strongest decrease in glacier volume was in sub-region R4 with an *APVC* of −1.04% ± 0.55% per year, and the weakest decrease appeared in region R1 with an *APVC* of −0.73% ± 0.77% per year (Table 1).

3.3. ELA change of glaciers

The *ELA* of each glacier was calculated using MEG and THAR, and the *ELAs* from the two methods were compared in the 1960s and 2010, respectively (Fig. 4). In the 1960s, the correlation coefficient (r) of MEG and ELA-THAR was above 0.97 (Fig. 4a), and the linear regression equation was $y = 0.95\times + 178.9$ ($R^2 > 0.95$, R^2 denotes the coefficient of determination; $p < 0.0001$, p denotes the significance level of statistic test). In 2010, the correlation coefficient was also above 0.97 (Fig. 4b), and the regression equation was $y = 0.93\times + 244.11$ ($R^2 > 0.95, p < 0.0001$). Hence, we confirmed that the MEG and ELA-THAR can be used as a practical alternative of *ELA* in the Chinese Tien Shan. In this paper, the arithmetic mean values of MEG and ELA-THAR were herein regarded as the *ELA* for each glacier in the 1960s and 2010, respectively.

The *ELA* shift of each glacier was calculated as shown in Fig. 5. In the 1960s, the mean *ELA* of the Chinese Tien Shan Mountains was 3970.35 ± 289.83 m a.s.l. (Table 1). In the sub-regions, the highest *ELA* of glaciers was located in sub-region R1 at 4402.86 ± 196.52 m a.s.l., while the lowest *ELA* was 3873.7 ± 187.91 m a.s.l. in sub-region R4. By 2010, the mean *ELA* of all glaciers in the Chinese Tien Shan Mountains increased to

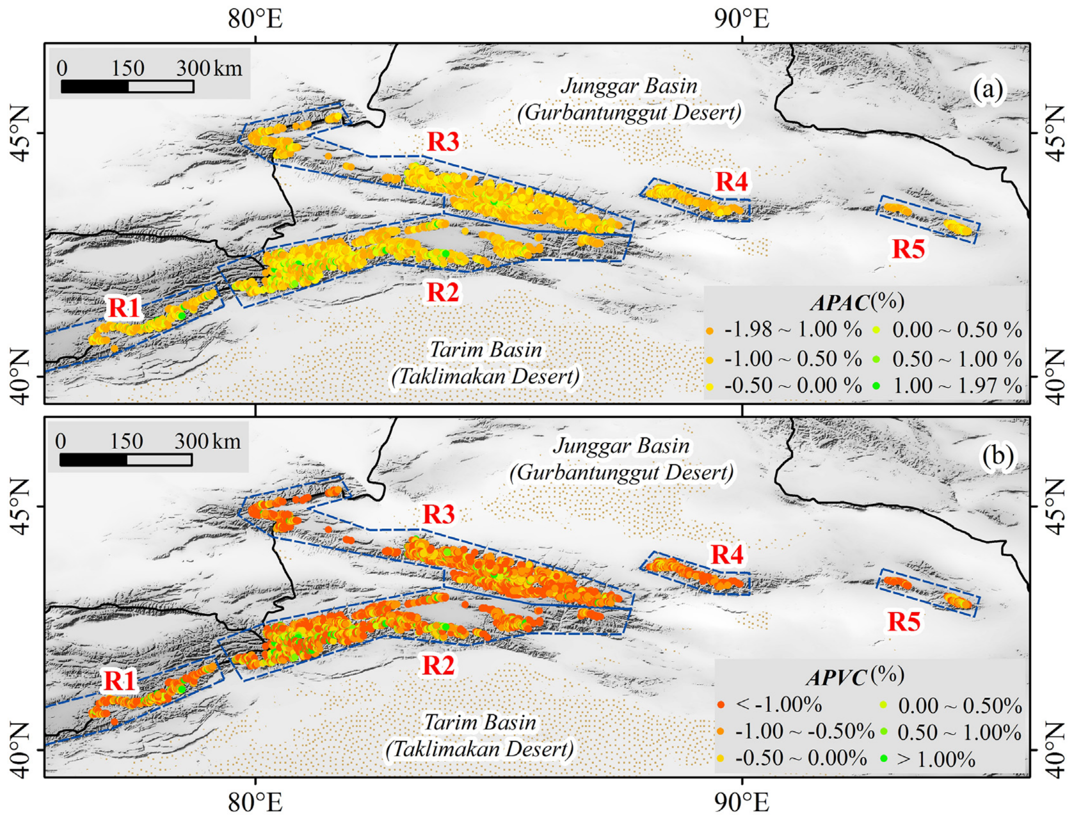

Fig. 3. Spatial distribution of the Annual Percentage of Area Change (*APAC*) (a) and Volume Change (*APVC*) (b) for each glacier in the Chinese Tien Shan Mountains from the 1960s to 2010. A negative value indicates glacier shrinkage.

3995.22 ± 257.56 m a.s.l. Similarly, the highest *ELA* of glaciers was in R1 at 4433.19 ± 180.36 m a.s.l., while the lowest *ELA* was 3918.05 ± 188.39 m a.s.l. in region R4. On the whole, the amount of glacier retreat in the Chinese Tien Shan accounted for 71.58%, and the amounts of glacier retreat in terms of area and volume were different, because they were different indictors of the response of glaciers to climate change and used the different methods. The mean *ELA* of glaciers in the Chinese Tien Shan increased by 24.87 ± 126.84 m a.s.l. during the period of the 1960s–2010.

The most significant change of glacier *ELA* was in R4 with Δ*ELA* of 44.35 ± 55.07 m. In addition, we obtained an obvious phenomenon, that is, the smallest Δ*ELA* of glaciers in the sub-regions was in region R2 with 13.23 ± 178.23 m, as shown in Table 1 and Fig. 5. Although the *ELA* of glaciers in sub-region R2 presented a state of relative stability, the *ELA* variation of each glacier was different. For example, some Δ*ELA*s were positive, i.e., the *ELA* of glaciers moved to higher elevation or glacier mass loss, while other Δ*ELA*s were negative, i.e., the *ELA* of glaciers moved to lower elevation or glacier mass increased. In addition, the largest standard deviation of 178.23 m partly accounted for this phenomenon. The changes in glacier area and volume also showed

Table 1

Descriptive statistics of the Arithmetic mean, standard deviation, maximum and minimum of Annual Percentage of Area Change (*APAC*) and Volume Change (*APVC*) from 1960s to 2010, *ELA* in 1960s (ELA_{1960s}) and 2010 (ELA_{2010}) and their difference ($\Delta ELA = ELA_{2010} - ELA_{1960s}$) in the Chinese Tianshan Mountains.

		Sub-region					Total
		R1	R2	R3	R4	R5	
APAC (%)	Mean	−0.61	−0.65	−0.72	−0.86	−0.66	−0.7
	St. Dev.	0.61	0.69	0.53	0.49	0.49	0.6
	Max	1.76	1.97	1.92	1.21	0.67	1.97
	Min	−1.93	−1.99	−1.91	−1.87	−1.79	−1.99
APVC (%)	Mean	−0.73	−0.76	−0.87	−1.04	−0.81	−0.83
	St. Dev.	0.77	0.85	0.63	0.55	0.58	0.73
	Max	2.77	3.13	3.05	1.84	0.98	3.13
	Min	−1.98	−2	−1.97	−1.95	−1.91	−2
ELA_{1960s} (m a.s.l.)	Mean	4402.86	3984.62	3898.83	3873.7	4044.74	3970.35
	St. Dev.	196.52	303.39	238.69	187.91	168.29	289.83
	Max	5584	6346	4860.9	4935.7	4471.8	6346
	Min	3405	3365.8	3228.5	3437.6	3678.1	3228.5
ELA_{2010} (m a.s.l.)	Mean	4433.19	3997.85	3929.43	3918.05	4078.12	3995.22
	St. Dev.	180.36	215.38	239.37	188.39	159.55	257.56
	Max	5403.1	5271.77	4781.87	4998.62	4435.19	5403.1
	Min	3973.42	3481.36	3258.66	3511.81	3747.31	3258.66
Δ*ELA* (m)	Mean	30.33	13.23	30.6	44.35	33.38	24.87
	St. Dev.	137.1	178.23	72.2	55.07	60.15	126.84

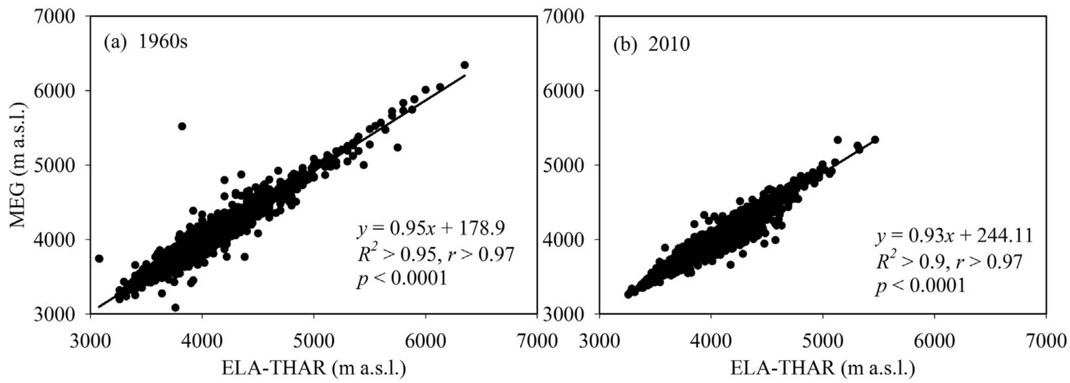

Fig. 4. Comparison of the Median Elevation of Glacier (MEG) with calculated *ELA* using THAR based on the datasets of CGI-1 in 1960s (a) and CGI-2 in 2010 (b) in the Chinese Tien Shan Mountains, respectively. In the plots, R^2 denotes the coefficient of determination, *r* denotes the correlative coefficient, and *p* denotes the significant level of the statistic test.

this pattern in space.

3.4. Climate change in glacierized regions

To interpret the glacier shrinkage in the Chinese Tien Shan, the climate change in the study region was analysed using the Mann-Kendall trend test (Kendall, 1975; Mann, 1945) and Sen's slope (Sen, 1968). The air temperature is an important indicator of glacier melting, and the glacier ablation generally occurs when the air temperature is higher than 0 °C (Braithwaite, 1995; Hock, 2005). In this study, the Thawing Degree-Day (TDD) and Freezing Degree-Day (FDD) were used as indexes of air temperature and calculated accordingly. Increasing positive TDD can accelerate glacier melting, while decreasing negative FDD is beneficial for glacier storage in cold environments. As shown in Figs. 6a and 7a, there were significantly increased trends ranging from 0.2 °C per year to 12.6 °C per year over the Chinese Tien Shan, and the trends of most grid cells were statistically significant at the 0.05 level. For the whole glacierized region, the increasing trend of TDD was very significant (Fig. 6e), and the mean TDD increased by 3.1 °C per year ($p < 0.001$) during the period of 1961–2010. In addition, FDD presented a significantly increased trend, except for some places (Figs. 6b and 7b), such as R4, most regions of central R2, and a part of eastern R3. However, the mean FDD presented a significantly increasing trend of 4.9 °C per year ($p < 0.01$) during 1961–2010 in the entire glacier region (Fig. 6f). In general, the increasing trends of TDD and FDD indicated that glacier melting in the Chinese Tien Shan was accelerating and that their protective effect from cold storage (i.e., the environment of low temperature) weakened during the past decades.

To understand the input of glacier mass, the precipitation amount (P) and the ratio of annual snowfall to total precipitation (S/P) were calculated in the Chinese Tien Shan. As shown in Fig. 6c, there were significantly increasing trends in the precipitation amount in northern regions of the Chinese Tien Shan (e.g., Junggar basin), while there was no significant trend in southern regions of the Chinese Tien Shan (e.g., Tarim Basin). In the sub-regions, there were large differences in terms of the trend of precipitation change (Fig. 6c and 7c). For instance, significant increases were only observed in the eastern mountains of R1 (Sen's slope > 3 mm/yr, $p < 0.05$), eastern mountains of R2 and R3 (Sen's slope > 1.5 mm/yr, $p < 0.05$), eastern mountains of R4 and western mountains of R5 (Sen's slope > 1 mm/yr, $p < 0.05$) (Fig. 6c). Additionally, the precipitation changes in other mountains were not significant at the 0.05 significance level. For annual precipitation in the whole glacierized region, however, there was a significantly increased trend from 1961 to 2010 with a slope of 1.2 mm/yr ($p < 0.01$) (Fig. 6g).

In addition, it is acknowledged that snowfall is very important to feed glaciers. Guo and Li (2015) found that the air temperature of 2 °C was a nice threshold to distinguish the snowfall and rainfall in the Chinese Tien Shan. Here, precipitation was defined as the snowfall when the daily mean air temperature was below 2 °C, and the S/P was calculated for each grid cell in the study region. Clear and significant trends were detected in terms of S/P in some grids of the glacierized region (Fig. 6d); for example, several grid cells of R2 and R3 showed a significantly decreasing trend in S/P. However, there was no significant trend detected in the annual S/P for the whole study region from 1961 to 2010 (Fig. 7h). In other words, although precipitation presented a

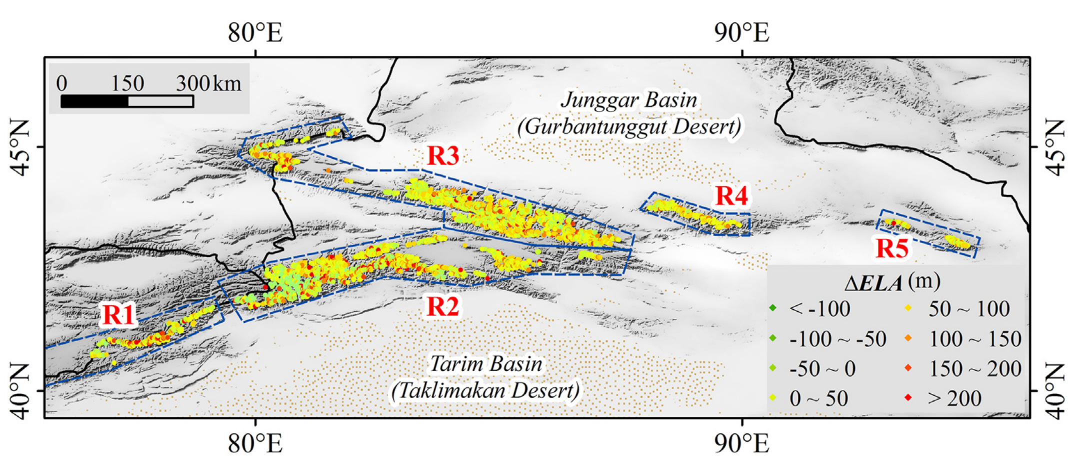

Fig. 5. The spatial distribution of the *ELA* variation (Δ*ELA*) of glaciers during the 1960s-2010 in the Chinese Tien Shan Mountains. The positive values denote an increasing *ELA*, while the negative values denote a decreasing *ELA*.

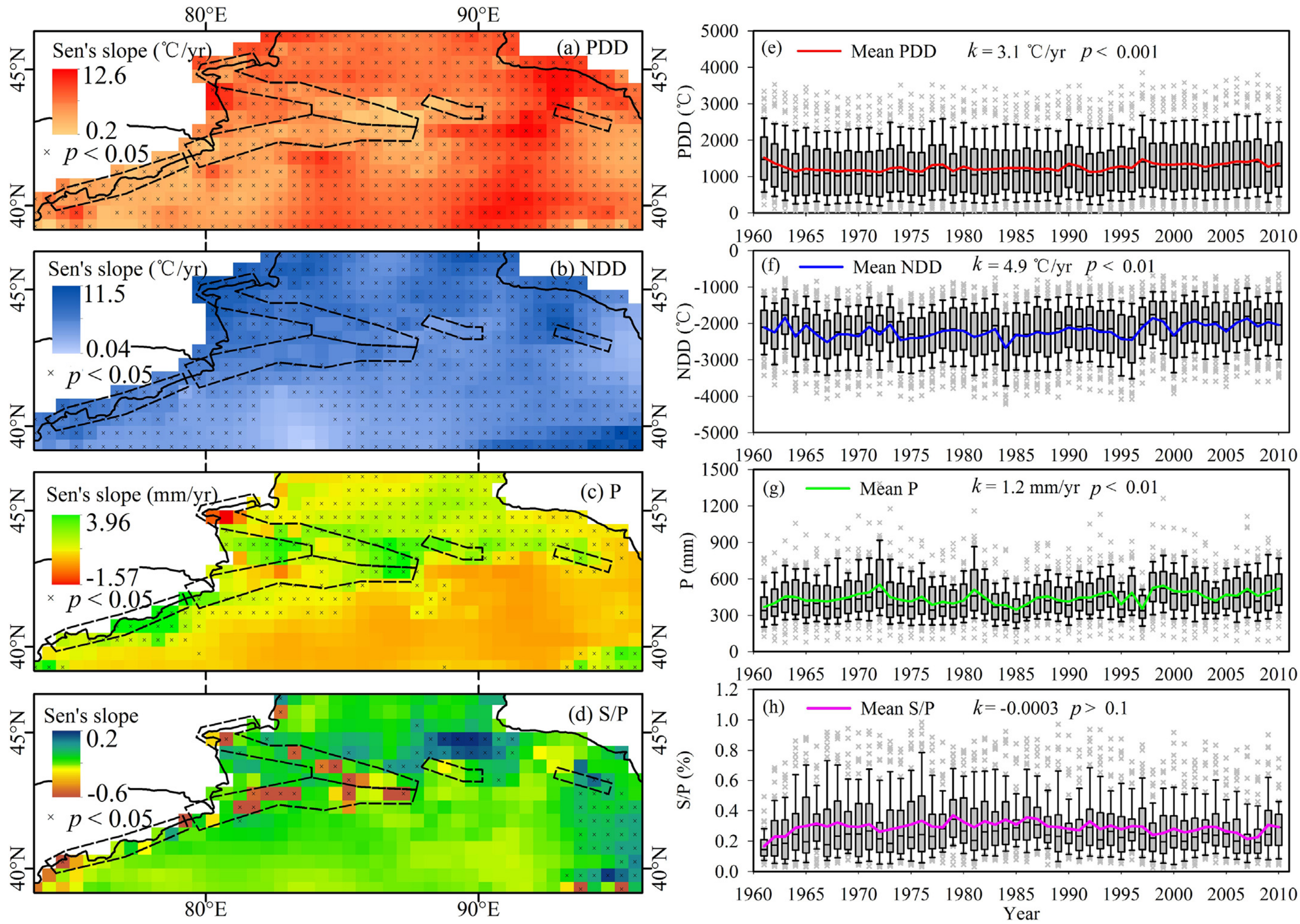

Fig. 6. (a)–(d) Spatial distribution of Sen's slopes of Thawing Degree-Day (TDD), Freezing Degree-Day (FDD), precipitation amount (P) and the ratio of snowfall to precipitation (S/P) from 1961 to 2010. Crosses in the grid cell centre represent that the slope is statistically significant at the 0.05 significance level using the Mann-Kendall methods. (e)–(h) Box plots of TDD, FDD, P and S/P in glacierized regions in all grid cells for each year from 1961 to 2010. The lower boundary of the box indicates the 25th percentile, the upper boundary of the box indicates the 75th percentile, a line within the box marks the 50th percentile (median), whiskers below and above the box present the 10th and 90th percentiles, respectively, and crosses below and above whiskers indicate outliers. The curves across the boxes denote the arithmetic mean of all grid cells in glacierized regions for each year. In addition, k denotes the slope, and p denotes the significant level of the statistic test.

significantly increasing trend, there was no significant trend for S/P in the Chinese Tien Shan.

4. Discussion

4.1. Glacier retreat in area

Based on the dataset of CGI-1 (1960s) and some references of glacier area change in the Chinese Tien Shan, including ~3000 glaciers, Wang et al. (2011b) indicated that the area-weighted *APAC* of glaciers decreased by 0.31% per year (the result was more reliable from 1960 to 1990–2006). Their work underestimated the rate of glacier shrinkage because they did not consider the different timespans of study works and used the same time period of 1960–2010, while most works had been conducted during the period of 1990–2006. Xu et al. (2015) found that the total glacial area decreased by ~0.6% per year in the Ili River Basin (mainly covering the inner region of western R2 and southwestern R3 in this paper) from the 1960s to late 2000s, which was similar to the results in R2 (−0.65% ± 0.69% per year) and R3 (−0.72% ± 0.53% per year) in this paper. Based on twelve glaciers with observed records located in nine river basins, Wang et al. (2015a, 2015b) noted that the larger changes in glacier area occurred in the Urumqi River Basin and Toutun River Basin in the central Chinese Tien Shan. The glacier area decreased by 0.83% per year and 0.77% per year during the period of 1964–2005 (corresponding to a glacier area reduction of 34.2% and 31.5% in total), respectively. The two basins are located in eastern R3 in this paper, and they had similar retreat rates in terms of the glacier area (Fig. 3a). In the Manas River Basin, i.e., located in the centre of region R3, the glacier area decreased by 0.6% per year during the period 1972–2013 (Xu et al., 2016). In the Bogda Mountains, i.e., region R4, the study on the change in glacier area was also conducted by Li et al. (2016), which indicated that the glacier area was reduced by 21.6% and that 12 glaciers vanished during the period of 1962–2006 (i.e., decreased by 0.5% per year). The glacier area on the southern slopes decreased by 25.3% during the period 1962–2006 (i.e., decreased by 0.58% per year), which was a stronger decrease than that on the northern slopes, which decreased by 16.9% (i.e., decreased by 0.38% per year), based on some investigated glaciers in the Bogda Mountains (Li et al., 2010; Wang et al., 2016a, 2016b).

In addition, the glaciers in different mountains of the Chinese Tien Shan showed different rates of glacier retreat from different studies, mainly ranging from −0.27% per year to −0.92% per year during the past several decades (He et al., 2013a, 2013b; He et al., 2015; Huai et al., 2014; Wang et al., 2009; Wang et al., 2014a, 2014b; Zhu et al., 2014). Even in the same region, the different studies from different research teams showed different retreat rates. For example, in the Ili

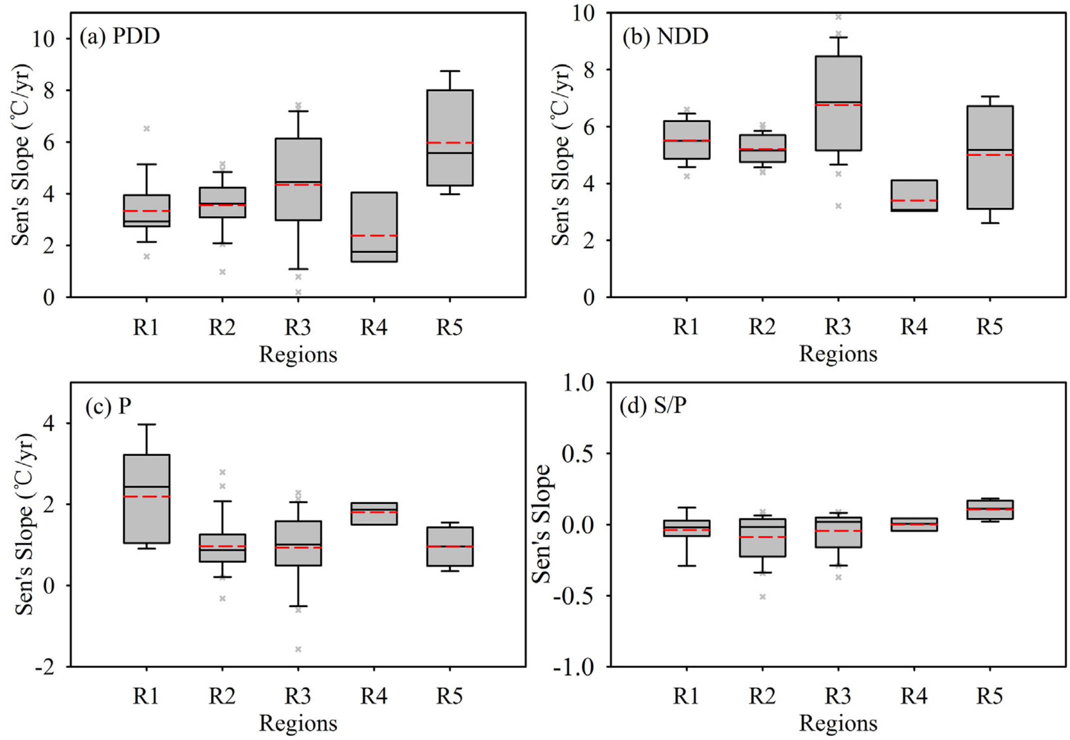

Fig. 7. Sen's slopes of climatic factors for sub-regions, including (a) Thawing Degree-Day (TDD), (b) Freezing Degree-Day (FDD), (c) Precipitation (P) and (d) Snowfall to Precipitation (S/P). In plots, the lower and upper boundaries of the box indicate the 25th and 75th percentiles, respectively. The black line within the box marks the 50th percentile (median), while the red line within the box marks the mean value of Sen's slope for all grid cells in each sub-region. The whiskers below and above the box present the 10th and 90th percentiles, respectively, and crosses below and above whiskers indicate outliers. (For interpretation of the references to colour in this figure legend, the reader is referred to the web version of this article.)

River Basin, Wang et al. (2011a, 2011b) presented a decreased area of approximately 0.2% per year, while Xu et al. (2015) noted that the glacier area decreased by ~0.6% per year, which mainly resulted from the different glacier datasets and discrepancies in the study periods that were used. The arithmetic mean of the *APAC* for glaciers in High Mountain Asia was −0.57% per year from 1960 to 2010 as described by Cogley (2016), who noted that the shrinkage rates were more negative than −0.8% and that relatively rapid shrinkage could be detected in the Tien Shan Mountains. In general, these studies have poor comparability in understanding the different patterns of glacier retreat in space. However, we used the glacier datasets of CGI-1 and CGI-2 and used closed timespans in this paper, and glaciers with uncertainty were removed (mentioned in " Section 2.2 Glacier Datasets"). Hence, we believed that the results of this paper were closer to the true values of glacier area change.

4.2. Glacier decrease in volume

The glacier volume was generally derived from field data, such as ground penetrating radar and borehole measurements (e.g., Bogorodsky et al., 1985; Flowers and Clarke, 1999). The measurements require several people to work together at the same time and come with relatively high costs; such measurements are not applicable to being extended into mountains. Therefore, there were only a few individual glaciers with a volume derived from field data (Radić and Hock, 2010). In the Chinese Tien Shan Mountains, Wang et al. (2012) assessed the volume change of six glaciers measured using ground penetrating radar, which showed that the volume decrease was much different. In addition, most of the observation was implemented in the ablation area, so volume data in terms of an entire glacier are still rare. Thus, more direct ice volume measurements are still needed to constrain the scaling parameters and further understand the glacier volume change in mountains.

4.3. Glacier changes in the different area sizes

The relative changes in small glaciers were usually higher than those of large ones with respect to the area changes, which indicated that the small glaciers were more sensitive to climate change than large glaciers (Knight, 1998; Nesje and Dahl, 2000; Wang et al., 2011a, 2011b). To understand the glacier retreat of different sized areas in the Chinese Tien Shan during the 1960s-2010, the glaciers were classified into ten groups, i.e., (0, 0.1], (0.1, 0.2], (0.2, 0.5], (0.5, 1], (1, 2], (2, 5], (5, 10], (10, 20], (20, 50], and (50, +∞). The changes in *APAC*, *APVC* and Δ*ELA* of each group were summarized as shown in Fig. 8. We found that the changes in the *APAC* of glaciers belonging to the groups of 0–10 km^2 were very significant. The *APACs* of glaciers belonging to groups of 10–50 km^2 were slightly positive. It was noted that of those glaciers, there were only 16 glaciers (Fig. 2) that had relatively large uncertainty due to limited samples. A similar pattern was shown in the *APVC* of different groups (Fig. 8c and d). With respect to the change in the *ELA* of different groups, the Δ*ELA* of small glaciers was also significant, especially the *ELAs* of glaciers smaller than 0.1 km^2, which rose by 27–38 m (Fig. 8e and f). In general, the retreat rates of small glaciers were more significant than those of large ones, that is, the small glaciers were more sensitive to climate change in the Chinese Tien Shan. However, the process of the response of glacier retreat to climate change was very complex, requiring a physical glacier-climate model for simulations and analysis (Ebrahimi and Marshall, 2016; Huss and Fischer, 2016; Zecchetto et al., 2016). For example, Zecchetto et al. (2016) revealed that the response time of a small glacier terminus to temperature was ~3.8 years in the Alps using the non-linear model.

4.4. Distribution of small glaciers

As mentioned above, small glaciers showed greater sensitivity than large ones in terms of climate change. We also found greater shrinkage

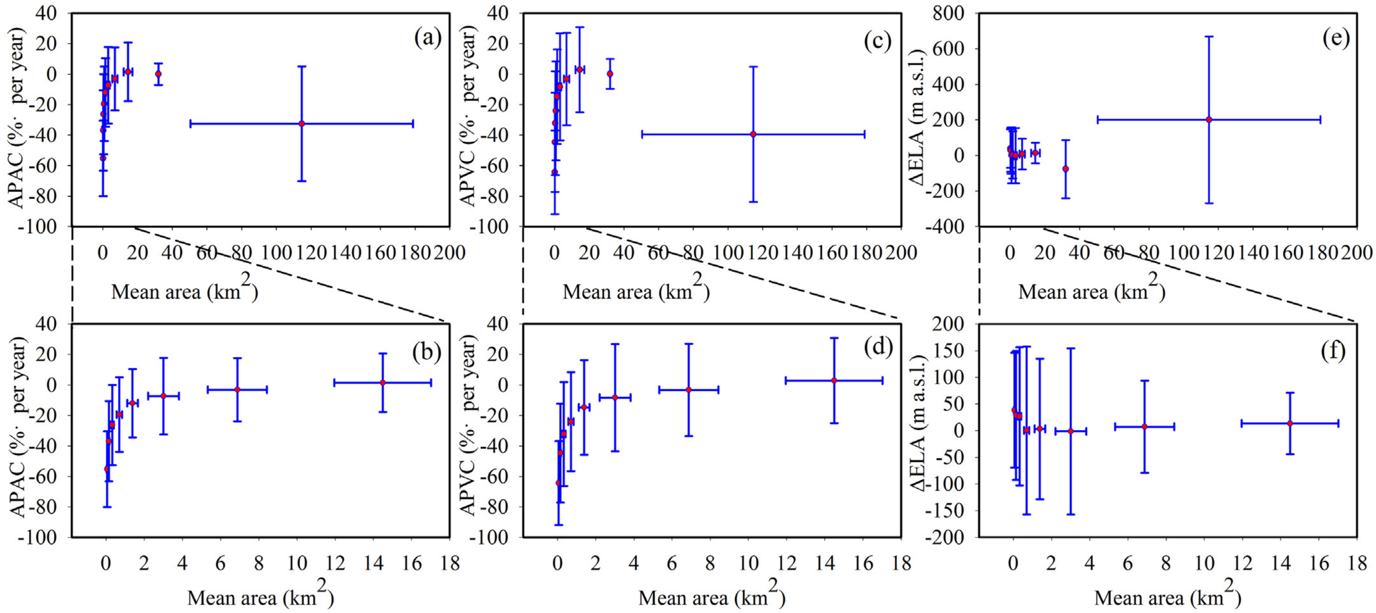

Fig. 8. Changes in *APAC*, *APVC* and Δ*ELA* of different groups with different sizes during 1960–2010. The glaciers were classified into ten groups according to their area, including the groups of (0, 0.1], (0.1, 0.2], (0.2, 0.5], (0.5, 1], (1, 2], (2, 5], (5, 10], (10, 20], (20, 50], and (50, $+\infty$), unit in km^2. The figures of the bottom panel zoomed in to the top panel with respect to the glaciers ranging from 0 to 18 km^2. In the bi-directional error bars, the red crossed points represent the arithmetic mean; the horizontal error bars denote the standard deviation of glacier area in each group; and the vertical error bars denote the standard deviation of glacier changes in each group. (For interpretation of the references to colour in this figure legend, the reader is referred to the web version of this article.)

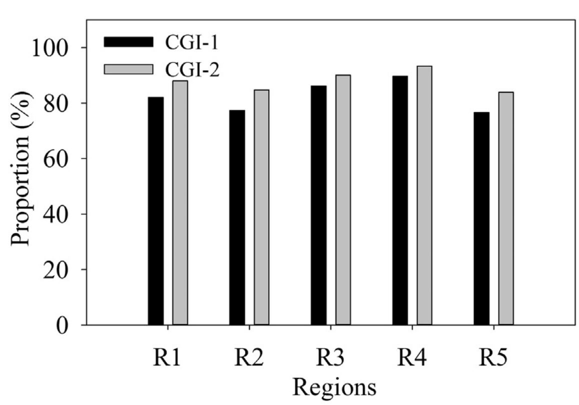

Fig. 9. The percentage of small glaciers $\leq 1\ km^2$ in sub-regions of the Chinese Tien Shan. "CGI-1" denotes the proportion of small glaciers in the first Chinese Glacier Inventory, and "CGI-2" denotes the proportion of small glaciers in the second Chinese Glacier Inventory.

in small glaciers than that in large ones in the Chinese Tien Shan. It was noted that the rate of glacial retreat in R4 (i.e., the Bogda Mountains) was the most significant, while the climate changes in the region were not the most significant compared with other regions. For example, the increase in the Sen's slope of TDD in R5 (i.e., the Harlik Mountains) was larger than that in the other four sub-regions (Fig. 7a), while the most significant increase in FDD was in R3 (North Chinese Tien Shan). That is, the increase in air temperature in R4 was the most significant, while the glaciers in this region showed the most significant retreat. To further understand this spatial discrepancy of glacial retreat in the Chinese Tien Shan, we compared the distribution of small glaciers $\leq 1\ km^2$ in the different sub-regions, as shown in Fig. 9. It was obvious that the percentage of small glaciers in R4 was larger than that in the other sub-regions (Fig. 9), with 89.70% and 93.35% in the CGI-1 and CGI-2, respectively. We deduced that the large rate of glacial retreat in R4 was mainly a result of the small glaciers. The increase in air temperature and lack of a significant increase in S/P were direct reasons for glacier shrinkage in the Chinese Tien Shan mountains.

5. Conclusions

It was accepted that the glaciers in the Chinese Tien Shan have widely retreated in the past several decades. In this paper, based on the datasets of the first and second Chinese Glacier Inventories (i.e., CGI-1 and CGI-2), the rates of glacier retreat in the Chinese Tien Shan were quantitatively assessed from the 1960s to 2010. The results indicated that the glacier area decreased on average by 0.7% ± 0.6% per year (i.e., *APAC* of −0.7% ± 0.6%) in the Chinese Tien Shan Mountains, and glacier volume decreased by 0.83% ± 0.73% per year (i.e., *APVC* of −0.83% ± 0.73%). The *ELA* of glaciers was distributed at 3970.35 ± 289.83 m a.s.l. of the Chinese Tien Shan in the 1960s and moved to 3995.22 ± 257.56 m a.s.l. in 2010. The *ELA* has risen on average by 24.87 ± 126.84 m during the period of the 1960s–2010. In sub-regions, the glacier shrinkage in R4 (i.e., the Bogda Mountains) was the most significant, with an *APAC* of −0.86% ± 0.49% per year and an *APVC* of −1.04% ± 0.55% per year, and the *ELA* increased by 44.35 ± 55.07 m from the 1960s to 2010.

In addition, to understand climate change in terms of glacier retreat in the Chinese Tien Shan, the TDD, FDD, P, and the ratio of S/P during the period of 1961–2010 were assessed. We found that there were significant increases in TDD and FDD during the study period, and the rates of increase were 3.1 °C per year ($p < 0.001$) and 4.9 °C per year ($p < 0.01$), respectively. There was no significant increasing trend in S/P, except for several grid cells, though a significant increasing trend existed in precipitation with a rate of increase 1.2 mm per year ($p < 0.01$). Hence, glacier retreat in the Chinese Tien Shan Mountains mainly resulted from the increase in the air temperature. In addition, the spatial discrepancies of glacier retreat in the different sub-regions were very significant, which was determined by both climate change and glacier characteristics, such as the air temperature, precipitation, snowfall, and glacier morphology (e.g., the distribution of small glaciers). Besides, to further understand the process between glacier

retreat and climate change, a glacier physical process model is needed in the future, and more field work will also need to be done.

Acknowledgements

We sincerely thank the Cold and Arid Regions of Science Data Center for providing the data of the first and second Chinese Glacier Inventory and thank the China Meteorological Data Sharing Service System for providing the meteorological data. This study was supported by the National Basic Research Program of China (973 Program) (No. 2013CBA01801), the National Natural Science Foundation of China (Nos. 41461003 and 41301069), the National Foundational Scientific and Technological Work Programs of the Ministry of Science and Technology of China (No. 2013FY111400), and the Foundation of the State Key Laboratory of Cryospheric Sciences (No. SKLCS-OP-2017-04).

References

Aa, A.R., 1996. Topographic control of equilibrium-line altitude depression on reconstructed 'Little Ice Age' glaciers, Grovabreen, western Norway. The Holocene 6 (1), 82–89.
Aizen, V.B., Aizen, E.M., Melack, J.M., 1995. Climate, snow cover, glaciers, and runoff in the tien Shan, Central Asia. Jawra J. Am. Water Res. Assoc. 31 (6), 1113–1129.
Aizen, V.B., Aizen, E.M., Melack, J.M., Dozier, J., 1997. Climatic and hydrologic changes in the Tien Shan, central Asia. J. Clim. 10 (6), 1393–1404.
Aizen, V.B., Kuzmichenok, V.A., Surazakov, A.B., Aizen, E.M., 2006. Glacier changes in the central and northern Tien Shan during the last 140 years based on surface and remote-sensing data. Ann. Glaciol. 43 (1), 202–213.
Bahr, D.B., 1997. Global distributions of glacier properties: a stochastic scaling paradigm. Water Resour. Res. 33 (7), 1669–1679.
Benn, D.I., Lehmkuhl, F., 2000. Mass balance and equilibrium-line altitudes of glaciers in high-mountain environments. Quat. Int. 65-66, 15–29.
Bishop, M.P., Olsenholler, J.A., Shroder, J.F., Barry, R.G., Raup, B.H., Bush, A.B.G., Copland, L., Dwyer, J.L., Fountain, A.G., Haeberli, W., Kääb, A., Paul, F., Hall, D.K., Kargel, J.S., Molnia, B.F., Trabant, D.C., Wessels, R., 2004. Global land ice measurements from space (GLIMS): remote sensing and GIS investigations of the Earth's cryosphere. Geocarto Int. 19 (2), 57–84.
Bogorodsky, V.V., Bentley, C.R., Gudmandsen, P.E., 1985. Radioglaciology. D. Reidel Publishing Company, Dordrecht, Holland.
Bolch, T., 2007. Climate change and glacier retreat in northern Tien Shan (Kazakhstan/Kyrgyzstan) using remote sensing data. Glob. Planet. Chang. 56, 1), 1–12.
Bothe, O., Fraedrich, K., Zhu, X., 2010. The large-scale circulations and summer drought and wetness on the Tibetan Plateau. Int. J. Climatol. 30 (6), 844–855.
Bothe, O., Fraedrich, K., Zhu, X., 2012. Precipitation climate of Central Asia and the large-scale atmospheric circulation. Theor. Appl. Climatol. 108 (3–4), 345–354.
Braithwaite, R.J., 1995. Positive degree-day factors for ablation on the Greenland ice sheet studied by energy-balance modelling. J. Glaciol. 41 (137), 153–160.
Braithwaite, R.J., Müller, F., 1980. On the Parameterization of Glacier Equilibrium Line Altitude. Vol. 126. IAHS Publ, pp. 263–271 (Riederalp Workshop 1978-World Glacier Inventory).
Braithwaite, R.J., Raper, S.C.B., 2009. Estimating equilibrium-line altitude (ELA) from glacier inventory data. Ann. Glaciol. 50 (53), 127–132.
Chen, J., Ohmura, A., 1990. Estimation of Alpine glacier water resources and their change since the 1870s. IAHS Publ. 193, 127–135.
Cogley, J.G., 2016. Glacier shrinkage across High Mountain Asia. Ann. Glaciol. 57 (71), 41–49.
Cui, H., Wang, J., 2013. The methods for estimating the equilibrium line altitudes of a glacier. J. Glaciol. Geocryol. 35 (2), 345–354 (in Chinese).
Ding, Y., Xie, Z., 1991. A simple method on estimating glacial mass balance. J. Glaciol. Geocryol. 13 (3), 213–218 (in Chinese).
Ding, Y., Liu, S., Li, J., Shangguan, D., 2006. The retreat of glaciers in response to recent climate warming in western China. Ann. Glaciol. 43 (1), 97–105.
Dong, L., Zhang, M., Wang, S., Zhu, X., Ren, Z., Wang, Q., 2014. Extreme precipitation events in arid areas in Northwest China based on gridded data. Journal of Natural Resources 29 (12), 2048–2057 (in Chinese).
Douglas, E.M., Vogel, R.M., Kroll, C.N., 2000. Trends in floods and low flows in the United States: impact of spatial correlation. J. Hydrol. 240, 90–105.
Ebrahimi, S., Marshall, S.J., 2016. Surface energy balance sensitivity to meteorological variability on Haig Glacier, Canadian Rocky Mountains. Cryosphere 10 (6), 2799–2819.
ElNesr, M.N., Abu-Zreig, M.M., Alazba, A.A., 2010. Temperature trends and distribution in the Arabian Peninsula. Am. J. Environ. Sci. 6, 191–203.
Erasov, N.V., 1968. Method to determine the volume of mountain glaciers. Mater. Glyatsiol. Issledovanii 14, 307–308.
Farinotti, D., Longuevergne, L., Moholdt, G., Duethmann, D., Mölg, T., Bolch, T., Güntner, A., 2015. Substantial glacier mass loss in the Tien Shan over the past 50 years. Nat. Geosci. 8, 716–723.
Flowers, G.E., Clarke, G.K.C., 1999. Surface and bed topography of Trapridge Glacier, Yukon territory, Canada: digital elevation models and derived hydraulic geometry. J. Glaciol. 45, 165–174.
Gardelle, J., Berthier, E., Arnaud, Y., 2012. Slight mass gain of Karakoram glaciers in the early twenty-first century. Nat. Geosci. 5(5), 322–325.
Gocic, M., Trajkovic, S., 2013. Analysis of changes in meteorological variables using Mann-Kendall and Sen's slope estimator statistical tests in Serbia [J]. Glob. Planet. Chang. 100 (1), 172–182.
Guo, L., Li, L., 2015. Variation of the proportion of precipitation occurring as snow in the tian Shan Mountains, China. Int. J. Climatol. 35 (7), 1379–1393.
Guo, W., Liu, S., Yao, X., Xu, J., Shangguan, D., Wu, L., Zhao, J., Liu, Q., Jiang, Z., Wei, J., Bao, W., Yu, P., Ding, L., Li, G., Li, P., Chunmei, G.E., Wang, Y., 2014. The second glacier inventory dataset of China (version 1.0). In: Cold and Arid Regions Science Data Center at Lanzhou, http://dx.doi.org/10.3972/glacier.001.2013.db.
Guo, W., Liu, S., Xu, J., Wu, L., Shangguan, D., Yao, X., Jiang, Z., 2015. The second Chinese glacier inventory: data, methods and results. J. Glaciol. 61 (226), 357–372.
Haeberli, W., 1998. Historical evolution and operational aspects of worldwide glacier monitoring. In: Haeberli, W., Hoelzle, M., Suter, S. (Eds.), Into the Second Century of Worldwide Glacier Monitoring: Prospects and Strategies. 56. UNESCO Studies and Reports in Hydrology, pp. 35–51.
Haeberli, W., Muller, P., Alean, P., Bosch, H., 1989. Glacier changes following the Little Ice Age - a survey of the international data basis and its perspectives. In: Oerlemans, J. (Ed.), Glacier Fluctuations and Climatic Change. Kluwer, pp. 77–101.
He, Y., Yang, T., Du, J., Tian, H., 2013a. Glacier variation of past 22 years in Alatau Mountains of Central Asia based on GIS and RS. Res. Soil Water Conserv. 20 (6), 130–134.
He, Y., Yang, T., Tian, H., Li, Z., 2013b. Response of glacier area variation to climate change in northern Tianshan Mountains in the past 23 years. J. Arid Land Res. Environ. 27 (3), 53–60.
He, Y., Yang, T., Ji, Q., Chen, J., Zhao, G., Shao, W., 2015. Glacier variation in response to climate change in Chinese Tianshan Mountains from 1989 to 2012. J. Mt. Sci. 12 (5), 1189–1202.
Hewitt, K., Young, G.J., 1990. Snow and Ice Hydrology Project: Upper Indus Basin. Overall Report. Canadian Centre.
Hock, R., 2005. Glacier melt: a review of processes and their modelling. Prog. Phys. Geogr. 29 (3), 362–391.
Hock, R., Jensen, H., 1999. Application of kriging interpolation for glacier mass balance computations. Geogr. Ann. 81 (4), 611–619.
Huai, B., Li, Z., Sun, M., Zhou, P., 2014. Glaciers change in the Tailan River watershed in the last 40 years. Sci. Geogr. Sin. 34 (2), 229–236 (in Chinese).
Huss, M., Fischer, M., 2016. Sensitivity of very small glaciers in the Swiss Alps to future climate change. Front. Earth Sci. 4, 34.
Immerzeel, W.W., Bierkens, M.F.P., 2012. Asia's water balance. Nat. Geosci. 5 (12), 841–842.
Immerzeel, W.W., van Beek, L.P.H., Bierkens, M.F.P., 2010. Climate change will affect the Asian water towers. Science 328 (5984), 1382–1385.
Immerzeel, W.W., Wanders, N., Lutz, A.F., Shea, J.M., Bierkens, M.F.P., 2015. Reconciling high-altitude precipitation in the upper Indus basin with glacier mass balances and runoff. Hydrol. Earth Syst. Sci. 19 (11), 4673.
Jansson, P., Hock, R., Schneider, T., 2003. The concept of glacier storage: a review. J. Hydrol. 282 (1), 116–129.
Kalesnik, S.V., 1963. Ocherki glaciologii Geografgiz. Moscow. (In Russian).
Kaser, G., Groÿhauser, M., Marzeion, B., 2010. Contribution potential of glaciers to water availability in different climate regimes. Proc. Natl. Acad. Sci. 107 (47), 20223–20227.
Kendall, M.G., 1975. Rank Correlation Methods. (Griffin, London).
Kenzhebaev, R., Barandun, M., Kronenberg, M., Chen, Y., Usubaliev, R., Hoelzle, M., 2017. Mass balance observations and reconstruction for Batysh Sook Glacier, Tien Shan, from 2004 to 2016. Cold Reg. Sci. Technol. 135, 76–89.
Knight, P.G., 1998. Glaciers. Stanley Thornes Ltd, Cheletenham.
Kraaijenbrink, P.D.A., Bierkens, M.F.P., Lutz, A.F., Immerzeel, W.W., 2017. Impact of a global temperature rise of 1.5 degrees Celsius on Asia's glaciers. Nature 549 (7671), 257–260.
Lettenmaier, D.P., Wood, E.F., Wallis, J.R., 1994. Hydro-climatological trends in the continental United States, 1948–88. J. Clim. 7, 586–607.
Li, B., Zhang, Y., Zhou, C., 2004. Remote sensing detection of glacier changes in Tianshan Mountains for the past 40 years. J. Geogr. Sci. 14 (3), 296–302.
Li, Z., Li, K., Wang, L., 2010. Study on recent glacier changes and their impact on water resources in Xinjiang, north western China. Quat. Sci. 30 (1), 96–106 (*in Chinese*).
Li, K., Li, Z., Gao, W., Wang, L., 2011. Recent glacial retreat and its effect on water resources in eastern Xinjiang. Chin. Sci. Bull. 56 (33), 3596–3604.
Li, K., Li, Z., Wang, C., Huai, B., 2016. Shrinkage of Mt. Bogda glaciers of eastern tian Shan in Central Asia during 1962–2006. J. Earth Sci. 27 (1), 139–150.
Lin, H., You, Q., Jiao, Y., Min, J., 2015. Spatial and temporal characteristics of the precipitation over the Tibetan plateau from 1961 to 2010 based on high resolution grid-observation dataset. J. Nat. Res. 30 (2), 271–281 *(in Chinese)*.
Liu, S., Yao, X., Guo, W., Xu, J., Shangguan, D., Wei, J., Bao, W., Wu, L., 2015. The contemporary glaciers in China based on the second Chinese glacier inventory. Acta Geograph. Sin. 70 (1), 3–16 (in Chinese).
Mann, H.B., 1945. Nonparametric tests against trend. Econometrica 13, 245–259.
Meier, M.F., Post, A.S., 1962. Recent Variations in Mass Net Budgets of Glaciers in Western North America. Publication-De l'As-Sociation Internationale d'Obergurgl. Vol. 58. pp. 63–77.
Meierding, T.C., 1982. Late Pleistocene glacial equilibrium-line altitudes in the Colorado Front Range: a comparison of methods. Quat. Res. 18 (3), 289–310.
Mukhopadhyay, B., Khan, A., 2017. Altitudinal variations of temperature, equilibrium line altitude, and accumulation-area ratio in Upper Indus Basin. Hydrol. Res. 48 (1), 214–230.
Murray, D.R., Locke III, W.W., 1989. Dynamics of the late Pleistocene big timber glacier,

Crazy Mountains, Montana, USA. J. Glaciol. 35 (120), 183–190.
National Meteorological Information Center (NMIC), 2012a. The Assessment Report of the Daily Air Temperature Datasets (SURF_CLI_CHN_TEM_DAY_GRID_0.5) at the Spatial Resolution of 0.5°×0.5°. *http://data.cma.cn/data/detail/dataCode/SURF_CLI_CHN_TEM_DAY_GRID_0.5/keywords/%E6%97%A5%E5%80%BC.html* (2016-11-30).
National Meteorological Information Center (NMIC), 2012b. The Assessment Report of the Daily Precipitation Datasets (SURF_CLI_CHN_TEM_DAY_GRID_0.5) at the Spatial Resolution of 0.5°×0.5°. *http://data.cma.cn/data/detail/dataCode/SURF_CLI_CHN_PRE_DAY_GRID_0.5/keywords/%E6%97%A5%E5%80%BC.html* (2016-11-30).
Nesje, A., Dahl, S.O., 2000. Glaciers and Environmental Change. Oxford University Press, New York.
Nie, Y., Zhang, Y., Liu, L., Zhang, J., 2010. Glacial change in the vicinity of Mt. Qomolangma (Everest), central high Himalayas since 1976. J. Geogr. Sci. 20 (5), 667–686.
Oerlemans, J., Anderson, B., Hubbard, A., Huybrechts, P., Johannesson, T., Knap, W.H., Schmeits, M., Stroeven, A.P., van de Wal, R.S.W., Wallinga, J., Zuo, Z., 1998. Modelling the response of glaciers to climate warming. Clim. Dyn. 14 (4), 267–274.
Osipov, E.Y., 2004. Equilibrium-line altitudes on reconstructed LGM glaciers of the northwest Barguzinsky Ridge, Northern Baikal, Russia. Palaeogeogr. Palaeoclimatol. Palaeoecol. 209 (1), 219–226.
Osmaston, H., 2005. Estimates of glacier equilibrium line altitudes by the area×altitude, the area×altitude balance ratio and the area×altitude balance index methods and their validation [J]. Quat. Int. 138-139, 22–31.
Østrem, G., Brugman, M., 1991. Glacier Mass-balance Measurements: A Manual for Field and Office Work. National Hydrological Research Institute, Saskatoon.
Partal, T., Kahya, E., 2006. Trend analysis in Turkish precipitation data. Hydrol. Process. 20, 2011–2026.
Pieczonka, T., Bolch, T., 2015. Region-wide glacier mass budgets and area changes for the Central Tien Shan between 1975 and 1999 using Hexagon KH-9 imagery. Glob. Planet. Chang. 128, 1–13.
Pieczonka, T., Bolch, T., W, J., Liu, S., 2013. Heterogeneous mass loss of glaciers in the Aksu-Tarim Catchment (Central Tien Shan) revealed by 1976 KH-9 Hexagon and 2009 SPOT-5 stereo imagery. Remote Sens. Environ. 130, 233–244.
Porter, S.C., 1981. Glaciological Evidence of Holocene Climatic Change. Climate and History, pp. 82–110.
Quincey, D.J., Braun, M., Glasser, N.F., Bishop, M.P., Hewitt, K., Luckman, A., 2011. Karakoram glacier surge dynamics. Geophys. Res. Lett. 38 (18) (L18504).
Radić, V., Hock, R., 2010. Regional and global volumes of glaciers derived from statistical upscaling of glacier inventory data. J. Geophys. Res. 115 (F1). http://dx.doi.org/10.1029/2009JF001373.
Radić, V., Hock, R., Oerlemans, J., 2007. Volume-area scaling vs flowline modelling in glacier volume projections. Ann. Glaciol. 46 (1), 234–240.
Radić, V., Hock, R., Oerlemans, J., 2008. Analysis of scaling methods in deriving future volume evolutions of valley glaciers. J. Glaciol. 54 (187), 601–612.
Ren, Z., Zhang, M., Wang, S., Qiang, F., Zhu, X., Dong, L., 2015. Changes in precipitation extremes in South China during 1961-2011. J. Geogr. Sci. 25 (1), 85–100.
RGI Consortium, 2017. Randolph Glacier Inventory-A Dataset of Global Glacier Outlines: Version 6.0: Technical Report, Global Land Ice Measurements from Space. Digital Media, Colorado, USA. http://dx.doi.org/10.7265/N5-RGI-60.
Sakai, A., Nuimura, T., Fujita, K., Takenaka, S., Nagai, H., Lamsal, D., 2015. Climate regime of Asian glaciers revealed by GAMDAM glacier inventory. Cryosphere 9 (3), 865–880.
Salami, A.W., Ikpee, O.D., Ibitoye, A.B., Oritola, S.F., 2016. Trend analysis of hydro-meteorological variables in the coastal area of Lagos using Mann-Kendall trend and standard anomaly index methods. J. Appl. Sci. Environ. Manag. 20 (3), 797.
Sen, P.K., 1968. Estimates of the regression coefficient based on Kendall's tau. J. Am. Stat. Assoc. 63 (324), 1379–1389.
Shen, X., Liu, B., Li, G., Zhou, D., 2015. Impact of climate change on temperate and alpine grasslands in China during 1982–2006. Adv. Meteorol. 1–10 ID 180614.
Shi, Y., Huang, M., Ren, B., 1988. An Introduction to the Glaciers in China. Science Press, Beijing (*in Chinese*).
Shi, Y., Liu, C., Kang, E., 2009. The glacier inventory of China. Ann. Glaciol. 50 (53), 1–4.
Sorg, A., Bolch, T., Stoffel, M., Solomina, O., Beniston, M., 2012. Climate change impacts on glaciers and runoff in Tien Shan (Central Asia). Nat. Clim. Chang. 2 (10), 725–731.
Tabari, H., Marofi, S., 2011. Changes of pan evaporation in the west of Iran. Water Resour. Manag. 25, 97–111.
Torsnes, I., Rye, N., Nesje, A., 1993. Modern and Little Ice Age equilibrium-line altitudes on outlet valley glaciers from Jostedalsbreen, Western Norway: an evaluation of different approaches to their calculation. Arct. Alp. Res. 25 (2), 106–116.
Viviroli, D., Dürr, H., Messerli, B., Meybeck, M., 2007. Mountains of the world, water towers for humanity: typology, mapping, and global significance. Water Resour. Res. 43 (W07447).
Wang, Y., Wang, J., Qi, Y., Yan, C., 2005. Dataset of Desert Distribution in China (1: 100,000). Environmental and Ecological Science Data Center for West China, National Natural Science Foundation of China, Lanzhou. http://dx.doi.org/10.3972/westdc.006.2013.db.
Wang, Y., Hou, S., Liu, Y., 2009. Glacier changes in the Karlik Shan, eastern Tien Shan, during 1971/72-2001/02. Ann. Glaciol. 50 (53), 39–45.
Wang, P., Li, Z., Gao, W., 2011a. Rapid shrinking of glaciers in the Middle Qilian Mountain region of Northwest China during the last ~50 years. J. Earth Sci. 22 (4), 539–548.
Wang, S., Zhang, M., Li, Z., Wang, F., Li, H., Li, Y., Huang, X., 2011b. Glacier area variation and climate change in the Chinese Tianshan Mountains since 1960. J. Geogr. Sci. 21 (2), 263–273.
Wang, P., Li, Z., Li, H., Wu, L., Jin, S., Zhou, P., 2012. Changes of ice-thickness and volume for representative glaciers in Tianshan Mountains in the past 50 years. Acta Geograph. Sin. 67 (7), 929–940 (in Chinese).
Wang, S., Zhang, M., Sun, M., Wang, B., Li, X., 2013. Changes in precipitation extremes in alpine areas of the Chinese Tianshan Mountains, Central Asia, 1961-2011. Quat. Int. 311, 97–107.
Wang, L., Li, Z., Wang, F., Edwards, R., 2014a. Glacier shrinkage in the Ebinur lake basin, Tien Shan, China, during the past 40 years. J. Glaciol. 60 (220), 245–254.
Wang, L., Li, Z., Wang, F., Li, H., Wang, P., 2014b. Glacier changes from 1964 to 2004 in the Jinghe River basin, Tien Shan. Cold Reg. Sci. Technol. 102, 78–83.
Wang, P., Li, Z., Huai, B., Wang, W., Li, H., Wang, L., 2015a. Spatial variability of glacial changes and their effects on water resources in the Chinese Tianshan Mountains during the last five decades. J. Arid Land 7 (6), 717–727.
Wang, X., Luo, Y., Sun, L., Zhang, Y., 2015b. Assessing the Effects of Precipitation and Temperature Changes on Hydrological Processes in a Glacier-Dominated Catchment. In: Hydrological Processes. Vol. 29(23). pp. 4830–4845.
Wang, J., Zhang, M., Wang, S., Ren, Z., Che, Y., Zhang, F., 2016a. Change of snowfall/rainfall ratio in the Tibetan Plateau based on a gridded dataset with high resolution during 1961–2013. J. Geogr. Sci. 26 (9), 1277–1288.
Wang, P., Li, Z., Wang, W., Li, H., Wu, L., Huai, B., Zhou, P., Jin, S., Wang, L., 2016b. Comparison of changes in glacier area and thickness on the northern and southern slopes of Mt. Bogda, eastern Tianshan Mountains. J. Appl. Geophys. 132, 164–173.
WGMS, National Snow and Ice Data Center (NSIDC), 1999. World Glacier Inventory, Version 1. [Indicate Subset Used]. Boulder, Colorado USA. NSIDC: National Snow and Ice Data Center. In: Doi, http://dx.doi.org/10.7265/N5/NSIDC-WGI-2012-02. updated 2012.
Wood, F.B., 1990. Monitoring global climatic change: the case of greenhouse warming. Bull. Am. Meteorol. Soc. 71 (1), 42–52.
Xie, Z., Ding, L., Liu, C., Liu, S., 1996. Mass balance at the steady state equilibrium line altitude and its application. J. Glaciol. Geocryol. 18 (1), 1–9 (*in Chinese*).
Xu, J., Liu, S., Guo, W., Zhang, Z., Wei, J., Feng, T., 2015. Glacial area changes in the Ili River catchment (Northeastern Tian Shan) in Xinjiang, China, from the 1960s to 2009. Adv. Meteorol. 1–12 ID847257.
Xu, C., Wang, F., Li, Z., Wang, L., Wang, P., 2016. Glacier variation in the Manas River Basin during the period from 1972 to 2013. Arid Zone Res. 33 (3), 628–635 (*in Chinese*).
Yang, Y., Tian, F., 2009. Abrupt change of runoff and its major driving factors in Haihe River catchment, China. J. Hydrol. 374 (3–4), 373–383.
Yao, T., Thompson, L., Yang, W., Yu, W., Gao, Y., Guo, X., Joswiak, D., 2012. Different glacier status with atmospheric circulations in Tibetan Plateau and surroundings. Nat. Clim. Chang. 2 (9), 663–667.
Zecchetto, S., Serandrei-Barbero, R., Donnici, S., 2016. Temperature reconstruction from the length fluctuations of small glaciers in the eastern Alps (northeastern Italy). Clim. Dyn. 1–12.
Zhang, M., Wang, S., Li, Z., Wang, F., 2011. Glacier area shrinkage in China and its climatic background during the past half century. J. Geogr. Sci. 22 (1), 15–28.
Zhao, Y., Zhu, J., 2015. Assessing quality of grid daily precipitation datasets in China in recent 50 years. Plateau Meteorol. 34 (1), 50–58 (in Chinese).
Zhu, W., Shangguan, D., Guo, W., Xu, J., 2014. Glaciers in some representative basins in the middle of the Tianshan Mountains: change and response to climate change. J. Glaciol. Geocryol. 36 (6), 1376–1384 (in Chinese).